Platinum and Molybdenum Oxide Supported on Mesostructured Silica Nanoparticles for *n*-Pentane and Cyclohexane Isomerization

Fatah, N.A.A.[1], Jalil, A.A. [1,2]*, Triwahyono, S. [3]

[1]Department of Chemical Engineering, Faculty of Chemical and Energy Engineering, Universiti Teknologi Malaysia, 81310 Johor Bahru, Johor, Malaysia
[2]Centre of Hydrogen Economy, Institute of Future Energy, Universiti Teknologi Malaysia, 81310 Johor Bahru, Johor, Malaysia
[3]Department of Chemistry, Faculty of Science, Universiti Teknologi Malaysia, 81310 Johor Bahru, Johor, Malaysia
Corresponding author: aishahaj@utm.my

Abstract

Alkane isomerization into its equivalent branched isomers has gained numerous attention as a reaction to obtain high quality fuel. In this study, platinum and molybdenum oxide supported on mesostructured silica nanoparticles (Pt/MoO$_3$/MSN) was prepared via impregnation method and tested for *n*-pentane and cyclohexane isomerization. The catalyst was characterized by using X-ray diffraction (XRD), nitrogen (N$_2$) physisorption, and pyridine Fourier-transform infrared (pyridine-FTIR) spectroscopy. The IR result revealed that the addition of Pt and MoO$_3$ into MSN formed different strength of Lewis and Brönsted acid sites. It was observed that the catalyst possessed strong acid sites and several numbers of relatively weak Lewis and Brönsted acid sites. Pt/MoO$_3$/MSN was catalytically active towards *n*-pentane and cyclohexane isomerization with conversion of 63 and 87%, respectively, at 300 °C. It was proposed that the addition of Pt might assist the generation of active protonic acid sites from molecular hydrogen via the mechanism of hydrogen spillover and hence improve isomerization reaction.

Keywords: Platinum, molybdenum oxide, mesostructured silica nanoparticles, isomerization.

1.0 INTRODUCTION

The growing level of environmental awareness contributes to strict regulations on aromatic compounds in gasoline content. Thus, catalytic isomerization of alkane gives a significant effect to increase the octane number of gasoline [1]. However, the practical application of this process has only been restricted to C$_4$/C$_6$ alkanes due to the undesirable cracking products obtained from the isomerization of long-chain alkanes [2]. Therefore, it is important to develop more efficient catalysts for the purpose of longer-chain alkane isomerization. Previously, many reports revealed that the addition of noble metals or transition metals on metal oxide, as well as microporous or mesoporous materials, gives high performance for isomerization of alkane [3, 4]. Among those supports, mesostructured silica nanoparticles (MSN) is a potential material for isomerization, which is attributed to its high surface area, as well as unique interparticle and intraparticle porosity. In recent years, molybdenum oxide (MoO$_3$) supported catalysts have been widely researched owing to their potential to catalyze linear alkane isomerization [5, 6]. It is noteworthy that the selectivity and activity of alkane isomerization catalysts are significantly influenced by the addition of noble metals such as platinum, palladium, and iridium. However, there is no report regarding platinum (Pt) and MoO$_3$ supported on MSN for the isomerization of *n*-pentane and cyclohexane. Therefore, in this study, Pt/MoO$_3$/MSN was tested for *n*-pentane and cyclohexane isomerization and its acidic property-catalytic activity relationship was investigated.

2.0 METHODOLOGY

2.1 Catalyst Preparation

MSN was synthesized by co-condensation and sol-gel methods according to the procedure in the literature [7]. 5 wt% of MoO$_3$ supported catalyst was prepared via incipient wetness impregnation of MSN with an aqueous solution of ammonium heptamolybdate solution ((NH$_4$)$_6$Mo$_7$O$_{24}$·4H$_2$O), followed by drying at 110 °C for 12 hr, and calcination in air at 550 °C for 3 hr. Pt/MoO$_3$/MSN was prepared via incipient wetness impregnation of MoO$_3$/MSN with an aqueous solution of hexachloroplatinic acid (H$_2$PtCl$_6$.H$_2$O), followed by drying at 110 °C for 12 hr, and calcination in air at 550 °C for 3 hr. The content of Pt was determined to be 0.5 wt%.

2.2   Characterization of Catalysts

The crystallinity of the catalysts was examined with X-ray diffraction (XRD) using a powder diffractometer (Bruker Advance D8, 40 kV, 40 mA) using Cu-Kα (λ = 1.5418 Å) radiation in the range of 2θ = 1.5–9.5°. A multiple-point Brunauer-Emmett-Teller (BET) gas adsorption analysis using an SA 3100 Surface Analyzer (Beckman Coulter) at -196 °C was carried out on all catalysts to determine their nitrogen adsorption-desorption isotherm. Prior to the analysis, evacuation procedure was performed on the sample at 300 °C for 1 hr.

Fourier-transform infrared (FTIR) analysis was performed using an Agilent Carry 640 FTIR spectrometer. Prior to the analysis, the catalysts were evacuated at 400 °C for 1 hr. In the adsorption of pyridine procedure, the catalysts were exposed to pyridine vapor at 150 °C and 2 torr for 15 min, followed by outgassing at 150 °C by a vacuum pump, and all spectra were obtained at room temperature [6].

2.3   Isomerization of *n*-Pentane and Cyclohexane

The isomerization of *n*-pentane and cyclohexane was carried out in a microcatalytic pulse reactor at 150–350 °C and analyzed by an online 6090N Agilent gas chromatograph equipped with a flame ionization detector (FID), VZ7 packed columns, and an FID detector. The conversion of reactant (X) was calculated by Equation 1:

$$X_{reactant} = \frac{\sum A_i - A_{reactant}}{\sum A_i}$$

(1)

where A_i is the corrected chromatographic area for a particular compound and $A_{reactant}$ corresponds to the chromatographic area of *n*-pentane and cyclohexane.

3.0 RESULTS AND DISCUSSION

3.1   Structural Properties

Fig. 1(a) shows the low-angle XRD patterns of pristine MSN and Pt/MoO$_3$/MSN. MSN showed three well-resolved Bragg diffraction peaks at 2θ = 2.2, 3.9, and 4.9°, which correspond to (100), (110), and (200) index of a typical two-dimensional hexagonally ordered mesostructure, demonstrating a high quality of mesopore arrangement [8]. The XRD pattern of Pt/MoO$_3$/MSN exhibited a significant decrease of peak at 2θ = 2.2°, suggesting that the long-range assembly of the mesoporous structure was reduced after the addition of Pt and MoO$_3$ metals. Although the crystallinity of the catalyst decreased, this is not the determining factor for catalyst deactivation [9]. Patel et al. reported that the lowest crystallinity of Co-MCM-41 showed the best activity as compared to other transition metals supported on MCM-41 in the reduction of NO with CO. Other factors may play important roles in the enhanced reaction such as metal-oxygen bond, acidity, and the role of metallic component.
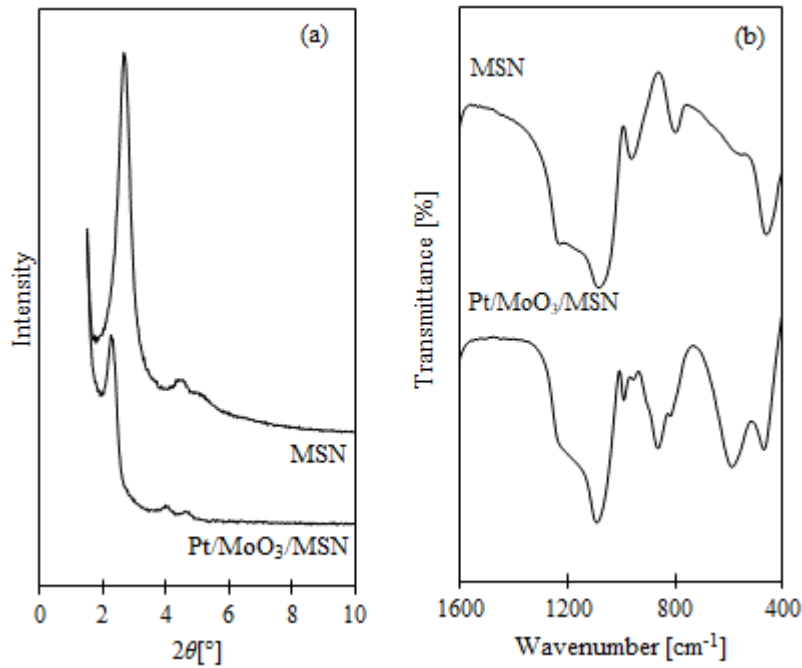
Figure 1. (a) XRD patterns and (b) IR spectra of catalysts

FT-IR analysis was carried out to distinguish the structural alterations of MSN after the addition of MoO_3 and Pt metal. Fig. 1(b) shows the IR spectra of MSN and $Pt/MoO_3/MSN$ in the array of 1600-400 cm^{-1}. MSN showed IR peaks at the bands attributed to Si-O-Si asymmetric stretching (1081 cm^{-1}), external Si-OH groups (946 cm^{-1}), Si-O-Si symmetric stretching (805 cm^{-1}), and Si-O-Si bending (455 cm^{-1}) [10]. Three additional bands were observed for $Pt/MoO_3/MSN$ spectrum, which correspond to Mo=O stretching mode (990 cm^{-1}), Mo-O-Mo (864 cm^{-1}), and Mo-O (586 cm^{-1}) [11]. Additionally, a band was observed at 820 cm^{-1}, which corresponds to vibrations of oxygen atoms associated to the orthorhombic structure of MoO_3 [12].
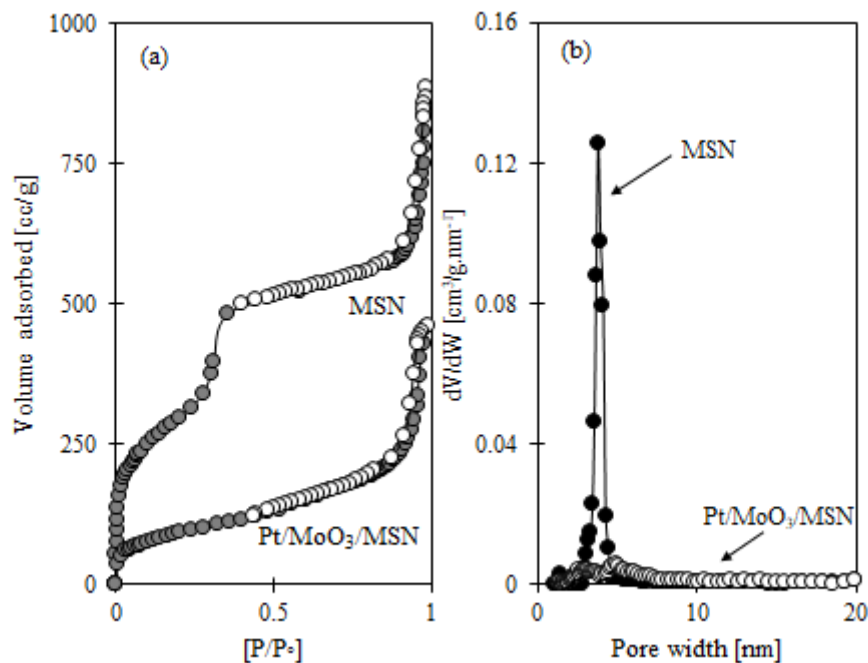

Figure 2. (a) N_2 adsorption-desorption isotherms and (b) pore size distribution of catalysts

The pore size distribution and nitrogen adsorption-desorption isotherms of MSN and Pt/MoO₃/MSN are shown in Fig. 2, whereas the textural parameters are presented in Table 1. Both catalysts showed a type IV isotherm that corresponds to the highly uniform cylindrical pores of mesoporous materials. Particularly, MSN exhibited two steps of capillary condensation at P/P_o = 0.3 and 0.9, which correspond to the intraparticles and interparticles inside mesopores [13]. The pore size distribution of MSN and Pt/MoO₃/MSN was monomodal, with an average pore width of 2.9 and 3.2 nm, respectively.

Table 1. Textural property of catalysts

Catalyst	Surface Area $(m^2/g)^a$	Total Pore Volume $(cm^3/g)^b$	Average Pore Size $(nm)^b$
MSN	1,118	0.764	2.9
Pt/MoO₃/MSN	879	0.796	3.2

^{a} Obtained from BET method
^{b} Obtained from non-local density functional theory (NL-DFT) method

The BET surface area of MSN and Pt/MoO₃/MSN demonstrated a deriving trend from 1,118 to 879 m^2/g with a slight increase of pore volume from 0.764 to 0.796 cm^3/g. The decrease in surface area could be attributed to the blockage of MSN pores by MoO₃ metal particles.

3.2 Acidic Properties of Catalysts

FTIR spectroscopy using pyridine as a probe molecule was employed to examine the nature of acid sites by identifying the absorbance band obtained between the interaction of the probe molecules and acidic sites. The FTIR spectra of pyridine adsorbed on Pt/MoO₃/MSN as a function of outgassing temperature after pyridine adsorption on activated catalyst are shown in Fig. 3. The catalyst showed an absorbance band at 1545 cm⁻¹ that corresponds to the C-N stretching of pyridinium ions ($C_5H_5NH^+$) bound to Brönsted acid sites on the catalyst surface, while the band at 1454 cm⁻¹ corresponds to the vibration of physically adsorbed pyridine that interacted with Lewis acid sites [6]. In this study, as the outgassing temperature increased, pyridine molecules adsorbed on weak acid should be desorbed at lower temperatures while those adsorbed on strong acid sites should be desorbed at higher temperatures.
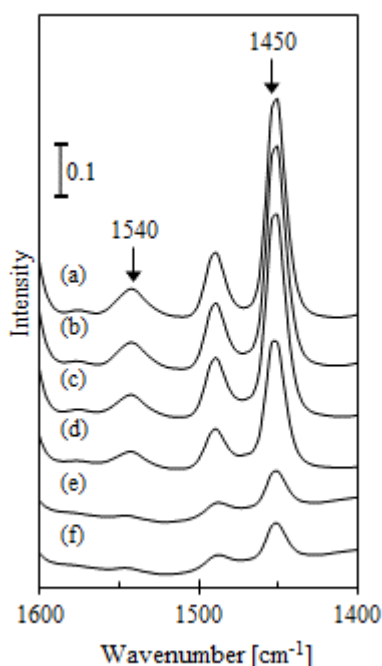

Figure 3. FTIR spectra of pyridine adsorbed on Pt/MoO₃/MSN evacuated at 400 °C, followed by pyridine adsorption at 150 °C and outgassing at (a) 150, (b) 200, (c) 250, (d) 300, (e) 350, and (f) 400 °C

Pt/MoO$_3$/MSN showed a significant decrease for both Brönsted and Lewis acid sites with increasing outgassing temperature from 150 to 400 °C. This result proposed the existence of extensive variation of both acidic sites in Pt/MoO$_3$/MSN. Particularly, an extensive decrease was observed on Brönsted acid sites compared to Lewis acid sites, suggesting that most of the Lewis acid sites on Pt/MoO$_3$/MSN were strong.

Fig. 4 shows the IR spectra of pyridine adsorbed on Pt/MoO$_3$/MSN at different activation temperatures. The catalysts were evacuated at 200, 250, 300, and 350 °C for 1 hr and the spectra were obtained after the adsorption reached an equilibrium at 150 °C, and the physisorbed state was subsequently eliminated by evacuating at 150 °C.
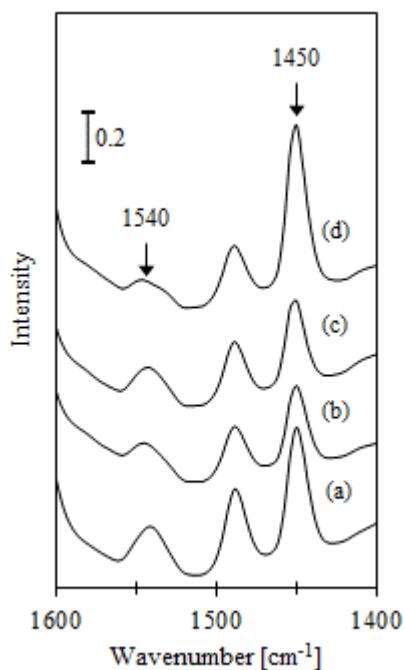

Figure 4. FTIR spectra of pyridine adsorbed on Pt/MoO$_3$/MSN samples activated at different temperatures. Samples were activated at (a) 200, (b) 250, (c) 300, and (d) 350 °C, followed by pyridine adsorption at 150 °C and outgassing at 150 °C

Therefore, the absorbance bands obtained can be evidenced as only strong adsorptions between the acidic sites and pyridine molecules. As the activation temperature raised, the absorbance bands at 1450 cm^{-1} increased while the bands at 1540 cm^{-1} decreased significantly. This result suggested that the Lewis acid sites were produced from the removal of surface hydroxyl groups at the same sites as protonic acid sites [5].

3.3 Catalytic Activity Performance

The catalytic activity of Pt/MoO$_3$/MSN catalyst in *n*-pentane and cyclohexane isomerization is shown in Fig. 5. It was observed that at reaction temperature below than 200 °C, the catalyst gave less than 40% conversion for both *n*-pentane and cyclohexane. At 300 °C, Pt/MoO$_3$/MSN showed a conversion of 63% and 87% for *n*-pentane and cyclohexane isomerization, respectively. Besides, the highest selectivity towards isomer products for both reactants was achieved at this reaction temperature. It is suggested that high Lewis acid sites in the catalyst may assist the production of active protonic acid sites originated from molecular hydrogen via hydrogen spillover mechanism [14]. The conversion for *n*-pentane and cyclohexane increased further at 350 °C, which was attributed to the formation of cracking products from thermal decomposition [15].
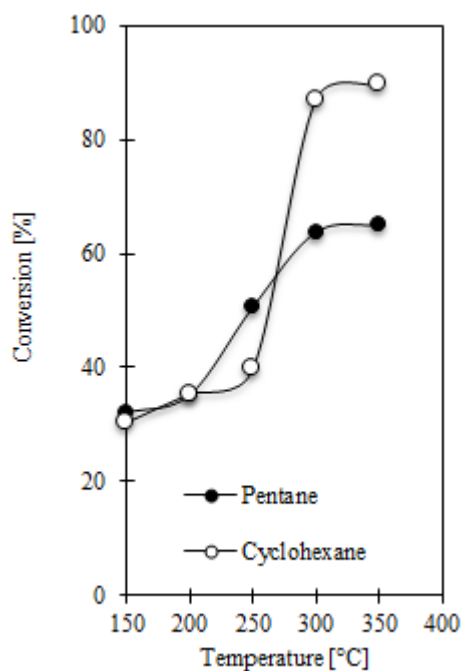
Figure 5. Conversion of *n*-pentane and cyclohexane over Pt/MoO$_3$/MSN in the presence of hydrogen

Previously, it has been reported that the production of protonic acid sites can be obtained when dissociated hydrogen molecules undergo surface dissociation to Lewis acid sites, followed by losing an electron to become a proton. The produced protonic acid sites give a significant role in alkane isomerization since the formation of carbenium ion should be initialized by the interaction between the reactant and protonic acid sites. Thus, it can be resolved that Pt/MoO$_3$/MSN is catalytically active for *n*-pentane and cyclohexane isomerization.

4.0 CONCLUSION

In this study, Pt/MoO$_3$/MSN was successfully prepared by impregnation of Pt and MoO$_3$ into MSN for *n*-pentane and cyclohexane isomerization. The XRD and BET results showed that the addition of Pt and MoO$_3$ in MSN reduced the crystallinity and surface area of MSN. The IR spectra of pyridine adsorbed on Pt/MoO$_3$/MSN showed that the catalyst consisted of strong acid sites and several numbers of relatively weak Lewis and Brönsted acid sites. The catalytic activity of Pt/MoO$_3$/MSN towards *n*-pentane and cyclohexane isomerization could be attributed from its acidic property to generate active protonic acid sites. It is proposed that the addition of Pt may assist the generation of active protonic acid sites from molecular hydrogen via hydrogen spillover mechanism.

References

[1]   Liu, P., Chang, W. T., Wang, J., Wu, M. Y., and Li, Y. X. 2015. MoP/Hβ catalyst prepared by low-temperature auto-combustion for hydroisomerization of *n*-heptane. *Catalysis Communications*, 66, 79-82.

[2]   Setiabudi, H. D., Jalil, A. A., and Triwahyono, S. 2012. Ir/Pt-HZSM5 for *n*-pentane isomerization: Effect of iridium loading on the properties and catalytic activity. *Journal of Catalysis*, 294, 128-135.

[3]   Al-Kandari, H., Al-Kharafi, F., and Katrib, A. 2009. Large scale hydroisomerization reactions of n-heptane on partially reduced MoO$_3$/TiO$_2$. *Applied Catalysis A: General*, 361(1), 81-85.

[4]   Annuar, N. H. R., Jalil, A. A., Triwahyono, S., Fatah, N. A. A., Teh, L. P., and Mamat, C. R. 2014. Cumene cracking over chromium oxide zirconia: Effect of chromium (VI) oxide precursors. *Applied Catalysis A: General*, *475*, 487-496.

[5]   Timmiati, S. N., Jalil, A. A., Triwahyono, S., Setiabudi, H. D., and Annuar, N. H. R. 2013. Formation of acidic Brönsted $(MoO_x)^-(H_y)^+$ evidenced by XRD and 2, 6-lutidine FTIR spectroscopy for cumene cracking. *Applied Catalysis A: General*, *459*, 8-16.

[6]   Ruslan, N. N., Triwahyono, S., Jalil, A. A., Timmiati, S. N., and Annuar, N. H. R. 2012. Study of the interaction between hydrogen and the MoO_3–ZrO_2 catalyst. *Applied Catalysis A: General*, *413*, 176-182.

[7]   Karim, A. H., Jalil, A. A., Triwahyono, S., Sidik, S. M., Kamarudin, N. H. N., Jusoh, R and Hameed, B. H. (2012). Amino modified mesostructured silica nanoparticles for efficient adsorption of methylene blue. *Journal of colloid and interface science*, *386*(1), 307-314.

[8]   Heikkilä, T., Santos, H. A., Kumar, N., Murzin, D. Y., Salonen, J., Laaksonen, T., and Lehto, V. P. 2010. Cytotoxicity study of ordered mesoporous silica MCM-41 and SBA-15 microparticles on Caco-2 cells. *European Journal of Pharmaceutics and Biopharmaceutics*, 74(3), 483-494.

[9]   Patel, A., Shukla, P., Rufford, T. E., Rudolph, V., and Zhu, Z. 2014. Selective catalytic reduction of NO with CO using different metal-oxides incorporated in MCM-41. Chemical Engineering Journal, 255, 437-444.

[10]   Kamarudin, N. H. N., Jalil, A. A., Triwahyono, S., Salleh, N. F. M., Karim, A. H., Mukti, R. R. and Ahmad, A. 2013. Role of 3-aminopropyltriethoxysilane in the preparation of mesoporous silica nanoparticles for ibuprofen delivery: Effect on physicochemical properties. *Microporous and Mesoporous Materials*, 180, 235-241.

[11]   Zakharova, G. S., Täschner, C., Volkov, V. L., Hellmann, I., Klingeler, R., Leonhardt, A., and Büchner, B. 2007. $MoO_3-\delta$ nanorods: Synthesis, characterization and magnetic properties. Solid State Sciences, 9(11), 1028-1032.

[12]   Ivanova, T., Surtchev, M., and Gesheva, K. 2002. Investigation of CVD molybdenum oxide films. Materials Letters, 53(4), 250-257.

[13]   Aziz, M.A.A., Jalil, A.A., Triwahyono, S., Mukti, R.R., Taufiq-Yap, Y.H., and Sazegar, M.R. 2014. Highly active Ni-promoted mesostructured silica nanoparticles for CO_2 methanation. *Applied Catalysis B: Environmental* (147) 359–368.

[14]   Triwahyono, S., Yamada, T. and Hattori, H. (2003). IR study of acid sites on WO_3–ZrO_2 and Pt/WO_3–ZrO_2 *Applied Catalysis A: General* (242) 101–109.

[15]   Kamarudin, N.H. N., Jalil, A.A., Triwahyono, S., Mukti, R.R., Aziz, M.A.A., Setiabudi, H.D., Muhid, M.N.M., and Hamdan, H. (2012). Interaction of Zn^{2+} with extraframework aluminum in HBEA zeolite and its role in enhancing *n*-pentane isomerization. *Applied Catalysis A: General,* (104) 431–432.